Available online at www.sciencedirect.com
SCIENCE DIRECT
Catalysis Today 113 (2006) 115–125
CATALYSIS TODAY
www.elsevier.com/locate/cattod

In situ MAS NMR studies of alkylaromatics transformations over acidic zeolites

Irina I. Ivanova [a,*], Nicolay S. Nesterenko [a], Christian Fernandez [b]

[a] Moscow State University, Department of Chemistry, Leninskie Gory, Moscow 119899, Russia
[b] Laboratoire Catalyse et Spectrochimie, Unité Mixte de Recherche CNRS/ENSICAEN/Université de Caen-Basse Normandie, 6 Bd. Maréchal Juin, 14050 Caen, France

Available online 6 January 2006

Abstract

The paper contains a short review on the impact of in situ ^{13}C and ^{1}H MAS NMR to the elucidation of the mechanisms of alkylaromatics transformation over zeolite catalysts. The studies of deuterated benzene and cumene transformations over protonic forms of zeolites are considered to account for the mechanisms of H/D exchange in the aromatic ring and alkyl chain. The investigations of ^{13}C label transfer in the course of the rearrangements of specifically labeled benzene, cumene, *n*-propylbenzene and ethylbenzene are reviewed to provide deeper insight in the mechanisms of transalkylation, disproportionation, skeletal and nonskeletal rearrangements of alkyl chain, fragmentation and dealkylation/alkylation over zeolites. The main factors controlling selectivity of zeolite catalysts in alkylbenzenes transformations are established.

Keywords: In situ MAS NMR; Transformation of alkylaromatics; Zeolites

1. Introduction

Alkylaromatic compounds have found a wide variety of applications in petrochemical and chemical industries as important intermediates in the production of commodity products such as polyesters, engineering plastics, detergents, pharmaceuticals, explosives, etc. Zeolites and zeolite-like materials were shown to be promising catalysts for conversion of alkylaromatics due to their high activity, selectivity, environmental safety and avoidance of corrosion [1–3]. Owing to the recent developments in the catalytic chemistry of zeolites, a drastic improvement in alkylaromatic conversion process technology has been achieved.

The future progress in this area requires a detailed knowledge of the mechanisms of catalytic transformations of alkylaromatics over zeolite catalysts. Therefore, this aspect of zeolite science received a considerable attention during the last years [4–29]. The mechanisms of alkylaromatic transformations over zeolite catalysts have been thoroughly studied using different experimental approaches: kinetic studies, theoretical calculations, etc. Besides that, many efforts have been put in the in situ spectroscopic investigations, which allow direct observation of the transformations of reactants and products during the time course of the reaction. Among the in situ spectroscopic techniques (IR, UV–vis, ESR and NMR), MAS NMR spectroscopy is considered to be one of the most informative [30–40] due to several reasons: (i) it provides the possibility to distinguish between different carbon atoms of the molecules and to identify unambiguously stable reaction intermediates; (ii) it allows for label tracing experiments with strategically ^{13}C and ^{2}D-labeled reactants, providing unique information on reaction mechanisms; (iii) it gives the possibility to obtain quantitative results and therefore to follow the kinetics of the reactions in situ.

The aim of this paper is to review in situ MAS NMR mechanistic studies of alkylbenzenes transformations over zeolite catalysts.

2. Experimental approaches used for in situ MAS NMR studies

At present, there are two general experimental protocols used to carry out in situ MAS NMR studies. The first one, which is used over the last 25 years, models catalytic experiments in a

* Corresponding author. Fax: +7 095 9328846.
E-mail address: IIIvanova@phys.chem.msu.ru (I.I. Ivanova).

0920-5861/$ – see front matter © 2005 Elsevier B.V. All rights reserved.
doi:10.1016/j.cattod.2005.11.016

batch reactor. In this approach, a catalyst and an adsorbate are introduced either in highly symmetrical sealed glass ampoules, fitting precisely into MAS rotors [41–47], or directly in gas tight MAS rotors [48–50]. In the latter case, special equipment is required for sealing and unsealing MAS rotors directly on a vacuum line [48–50].

The second, relatively recent experimental approach, allows carrying out in situ MAS NMR investigations under continuous flow conditions. There are several different designs reported, which allow for such experiments [51–56]. All of them imply reactants injection with carrier gas into the MAS rotor with a catalyst directly in the NMR spectrometer.

The detailed description of the techniques used for both batch and flow experiments is given in the other reviews [30,31,35,38,50,56]. In this paper, we review the results of in situ MAS NMR studies of alkylbenzenes transformations over zeolite catalysts, which were preferentially obtained using the first experimental approach.

3. H/D exchange

The easiest reaction, which takes place already at ambient temperature upon adsorption of alkylaromatic compounds, is the exchange between the acidic protons of zeolite and the protons of the aromatic ring. This was demonstrated by in situ ^{1}H MAS NMR study of H/D exchange during the reactions of deuterated benzene [57] and deuterated cumene [58] over various zeolite catalysts.

As depicted in Fig. 1, the initial spectrum of partially exchanged mordenite (HNaMOR) exhibited two NMR lines at ca. 4.2 and 2.0 ppm. The first one was attributed to bridging hydroxyls (Si–OH–Al), while the second was assigned to silanol groups (Si–OH). Upon adsorption of deuterated cumene, the intensity of the line corresponding to bridging hydroxyl groups decreased and at the same time two intensive lines at ca. 7.0 and 7.4 ppm, corresponding to the protons in the aromatic ring of cumene, appeared. The broad line (7.4 ppm) was attributed to less mobile species constrained in the zeolite channels, while the narrow line (7.0 ppm) to more mobile species [58]. The weak resonances at ca. $\delta = 1$ and 2.5 ppm were due to the residual protons in the methyl and methyne groups of cumene, contained in starting deuterated cumene. The increase of the reaction time (40, 80 and 120 min) resulted in gradual decrease of the intensity of the line corresponding to bridging hydroxyls and the increase of the lines ascribed to aromatic protons, while the protons of silanol groups did not take part in the reaction. After about 10 h of reaction, the H/D exchange between the deuterium atoms in the aromatic ring of cumene and the acidic protons reached equilibrium and no further changes were observed at ambient temperature.

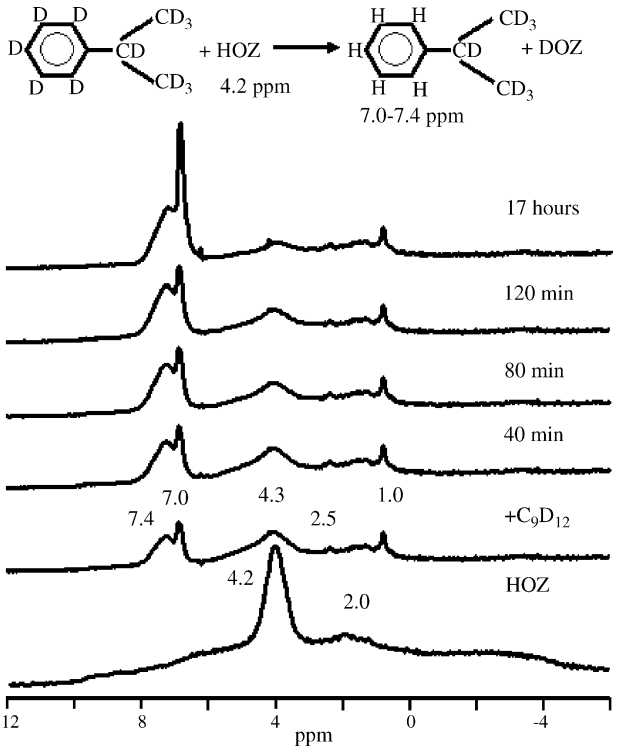

Fig. 1. ^{1}H MAS NMR spectra obtained before and during the reaction of deuterated cumene on HNaMOR zeolite at ambient temperature [58].

The investigation of H/D exchange during cumene interaction with fully exchanged (H-MOR) and dealuminated mordenite (H-DealMOR) pointed to even faster reaction. Thus, on H-MOR, the reaction was completed after 45 min, while on H-DealMOR, it was completed immediately after adsorption. This could be due to either higher acidity or better accessibility of the acidic sites in the channels of fully exchanged and dealuminated mordenites.

Beck et al. [57] used temperature-jump NMR experiments to measure the activation energies for H/D exchange between the acidic protons in various zeolites and benzene-d_6. Initial rate data were fitted to Arrhenius plots that yielded activation energies ranging between 14.4 and 25.5 kcal/mol (Fig. 2). These values are in good agreement with the theoretical barrier (20.3 kcal/mol) obtained using density functional theory for calculation of H/D exchange through concerted mechanism depicted in Fig. 3. According to this mechanism, H/D exchange

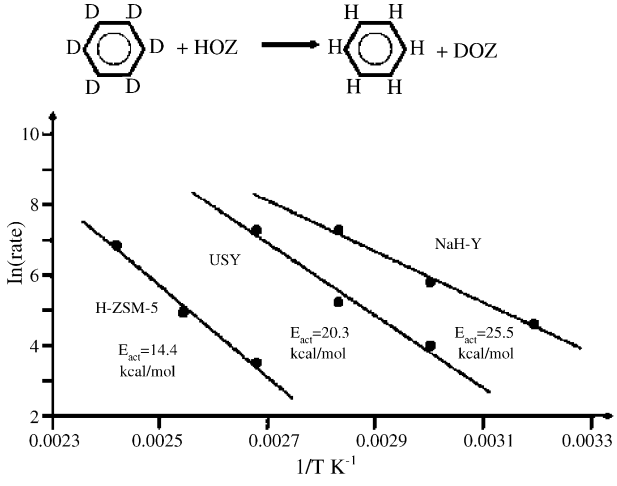

Fig. 2. Arrhenius plots constructed from in situ H-ZSM-5, USY and NaHY kinetics studies of H/D exchange between zeolitic protons and benzene-d_6 at various temperatures [57].

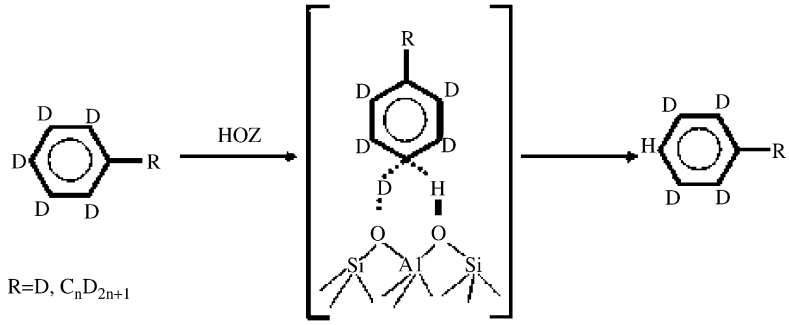

Fig. 3. Mechanism of H/D exchange in the aromatic ring of alkylaromatic compounds over zeolite catalysts.

occurs via a concerted cleavage of O–H bond in zeolitic bridging OH group and formation of O–D bond between deuterium atom of aromatic ring and the neighboring oxygen of zeolite.

While H/D exchange in the aromatic ring readily occurred at ambient temperature, no exchange was observed in the alkyl chain even at longer reaction times. Indeed, the intensities of the lines at ca. 1 and 2.5 ppm did not change in the spectra presented in Fig. 1. The hydrogen atoms of the alkyl chain started to participate in the H/D exchange only at elevated temperatures: at 393 K over H-DealMOR, at 433 K over H-MOR and only at 473 over HNaMOR [58]. The results obtained over H-DealMOR catalyst are presented in Fig. 4. Upon heating the sample to 393 K, the intensity of the line corresponding to methyl group protons started to increase. Heating at 433 and 473 K resulted in further intensity enhancement of this line. It is worth noting that no H/D exchange was observed in methyne group of cumene, as evidenced by no enhancement of the NMR line at ca. 2.5 ppm (Fig. 4). The selective H/D exchange in the methyl group of alkyl chain was explained by propylene intermediate formation [58] as depicted in Fig. 5. Indeed, according to Markovnikov rule, zeolite protons should exchange with methylene groups of propylene, which are further converted into methyl groups of cumene upon alkylation.

To summarize, in situ ^{1}H MAS NMR results concluded to a concerted mechanism of H/D exchange in the aromatic ring and pointed to dealkylation/alkylation mechanism of H/D exchange in the alkyl chain.

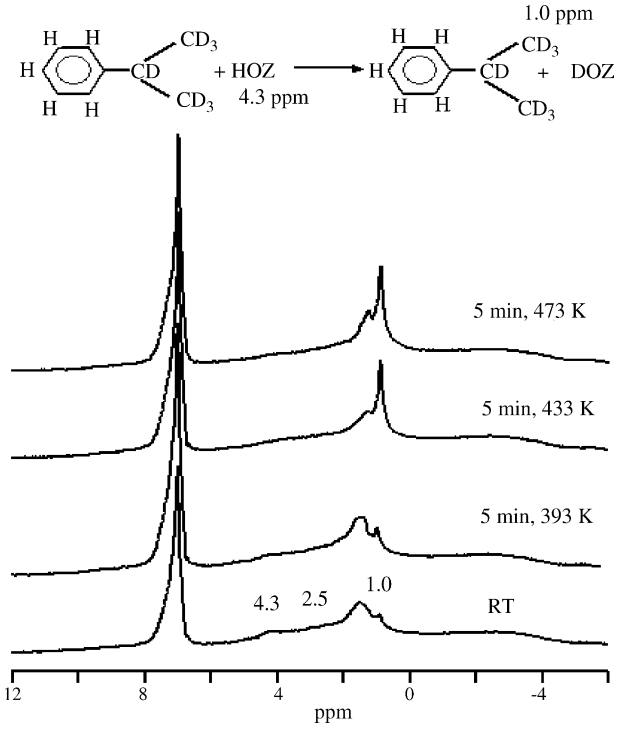

Fig. 4. ^{1}H MAS NMR spectra observed during the reaction of deuterated cumene at elevated temperatures over HDealMOR catalyst [58].

4. Transalkylation and disproportionation

The next reaction step includes transalkylation and disproportionation of alkylaromatics. Three mechanisms have been proposed in the literature to account for these types of reactions over zeolite catalysts [4,5]:

- The first one included the shift of the alkyl group from one aromatic ring to another without intermediate formation of a free alkyl carbocation [5].
- The second one involved dealkylation/alkylation S_{N1} mechanism, in which alkyl carbenium ions were supposed as intermediates [6,20].
- Finally, the third one assumed S_{N2} mechanism involving bimolecular intermediates, in which aromatic rings are bridged by a C atom of the alkyl group. Two substrate activation routes over zeolite type catalysts were suggested in the literature for this mechanism: hydride abstraction resulting in formation of

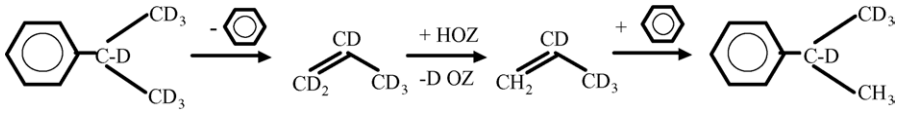

Fig. 5. Mechanism of H/D exchange in the alkyl chain of cumene over zeolites.

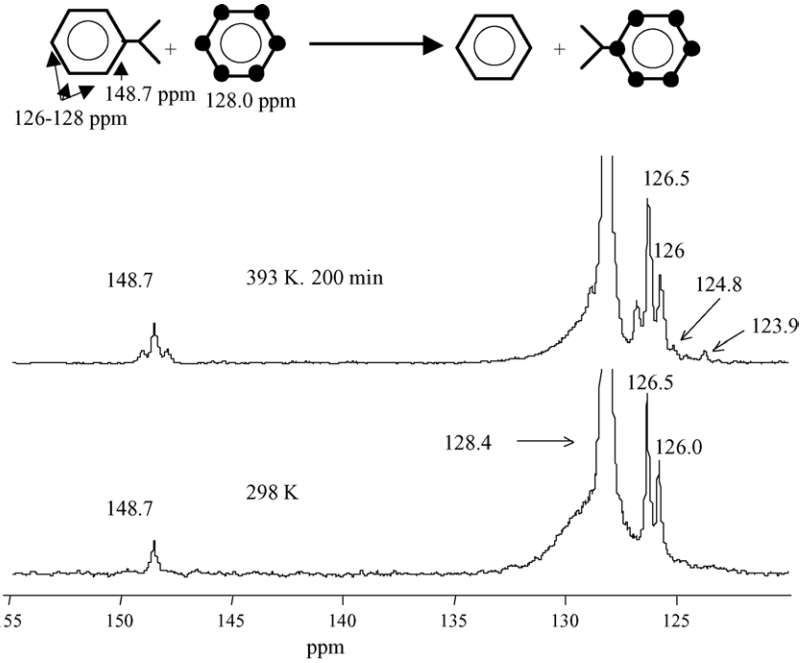

Fig. 6. Aromatic region of ^{13}C MAS NMR spectra observed before and after the reaction of benzene-^{13}C and unlabeled cumene over HMOR catalyst [61].

benzylic carbocations [4,5,7,8,20,59] and protonation of the aromatic ring with subsequent rearrangement of the benzenium ion towards a primary carbocation [5,6].

An in situ ^{13}C MAS NMR technique has been applied for the investigation of transalkylation of cumene with diisopropylbenzene [60–62] and disproportionation of ethylbenzene [63]. It has been demonstrated that these types of reactions start on zeolitic catalysts in the temperature region of 293–473 K depending on zeolite acidity and reaction type.

To follow the transalkylation of benzene with isopropylbenzene, benzene was initially labeled with ^{13}C isotope and the reaction was carried out on two types of zeolites: large pore mordenite [61] and medium pore H-ZSM-11 [60,62].

The typical initial ^{13}C MAS NMR spectrum obtained immediately after adsorption of the reactants on fully exchanged mordenite showed an intense line at 128.4 ppm corresponding to ^{13}C labeled carbon atoms of benzene and five low intensity peaks at 126.0, 126.5 and 148.7 ppm corresponding to unlabeled aromatic carbon atoms of cumene (Fig. 6). Heating at 393 K resulted in the splitting of the aromatic cumene peaks into triplets due to ^{13}C–^{13}C scalar coupling (J_{CC} = 55 Hz) in the aromatic ring of cumene. Since ^{13}C–^{13}C coupling could occur only in labeled cumene, the result points to a transalkylation reaction between unlabeled cumene and labeled benzene on H-MOR catalyst at 393 K. Besides splitting, two new ^{13}C NMR lines were observed at 123.9 and 124.8 ppm. These new lines were assigned to diisopropylbenzene and evidenced that disproportionation of cumene occurs in parallel to the transalkylation route. On dealuminated mordenite, these transformations started already at ambient temperature, while on partially exchanged mordenite (HNa-MOR) the transalkylation and disproportionation reactions began only at 473 K. Since the acidic strength of the mordenite did not change significantly upon dealumination, the extremely high activity of the dealuminated MOR was explained by the

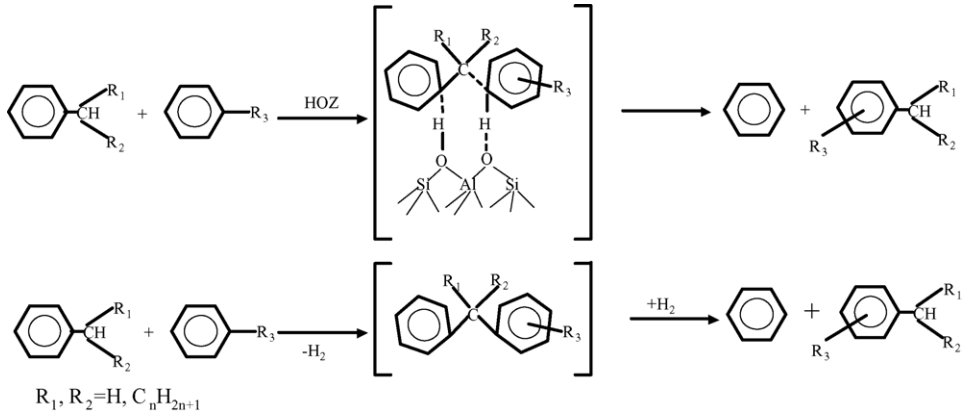

Fig. 7. Mechanisms of alkylbenzenes transalkylation over acidic zeolites.

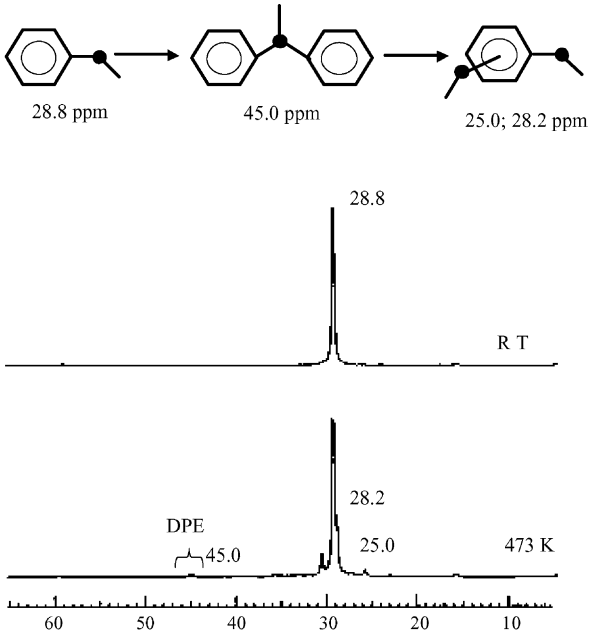

Fig. 8. ^{13}C MAS NMR spectra observed before and after the reaction of ethylbenzene α-^{13}C at 473 K over Pt-HMOR [63].

creation of secondary mesoporosity, which favors the formation of reaction intermediate.

It is important to note that transalkylation and disproportionation reactions were not observed during a study of cumene interaction with labeled benzene over H-ZSM-11 using the same experimental technique [60,62]. This could be explained by the space restrictions for the formation reaction intermediate in medium pore zeolites.

All these data pointed that transalkylation and disproportionation reactions proceed via formation of bulky intermediate, which can be easily formed in dealuminated mordenite and is restricted in H-ZSM-11. It was thus suggested that disproportionation of cumene and transalkylation of cumene and benzene proceed either via propyl shift involving concerted formation of bulky transition state shown in Fig. 7 or via intermolecular S_{N2} mechanism including the formation of bulky 2,2-diphenylpropane intermediate.

Another evidences for the intermolecular S_{N2} mechanism of disproportionation of alkylaromatic compounds were obtained in ^{13}C MAS NMR study of ethylbenzene transformations over mordenite catalysts [63]. In this study, ethylbenzene enriched with ^{13}C isotope in the α-position of the side chain was used as a starting reactant. The only products observed at the initial step of the reaction (at 473 K) were *para- and ortho*-diethylbenzenes retaining the label at the α-position of the side chain (Fig. 8). No diethylbenzenes with the label in the β-position were observed at this reaction step, what excluded the possibility of dealkylation/alkylation mechanistic pathway, requiring statistical distribution of ^{13}C label. This led the authors to the conclusion that ethylbenzene disproportionation occurs via bimolecular S_{N2} mechanism involving 2,2-diphenylethane (DPE) as an intermediate. This intermediate was further detected on mordenite catalyst modified by Pt (Fig. 8). The longer lifetime of the intermediate on the later catalyst was most probably due to the ability of Pt to retain dihydrogen. It should be mentioned, however, that these observations do not exclude the possibility of alkyl shift mechanism.

Consequently, two mechanisms were proposed to account for transalkylation and disproportionation of alkylaromatics over zeolite catalysts: intermolecular S_{N2} mechanism involving bimolecular intermediates, in which aromatic rings are bridged by a C atom of the alkyl group, and concerted mechanism of alkyl shift involving eight member cyclic transition state.

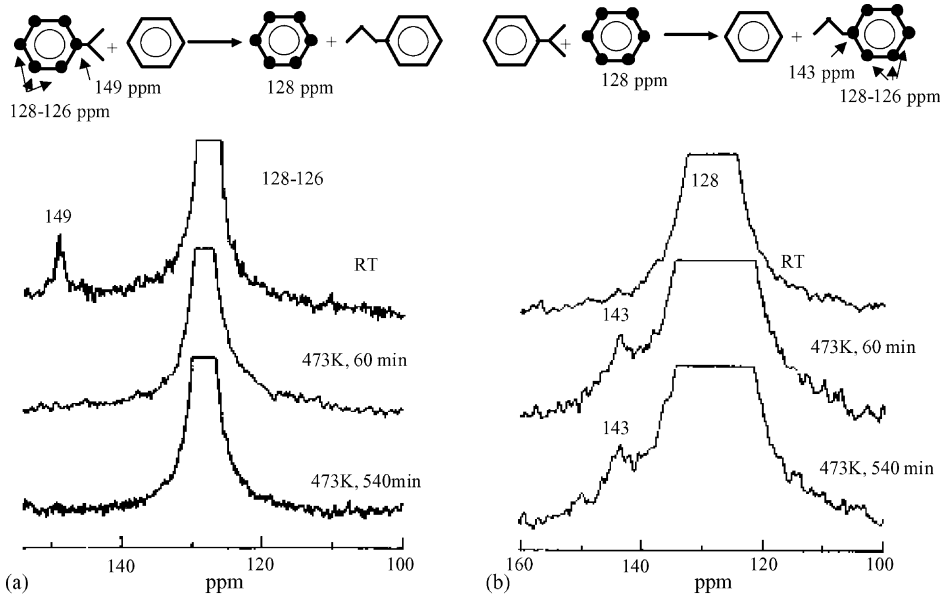

Fig. 9. Aromatic regions of ^{13}C MAS NMR spectra observed before and during the reaction at 473 K of unlabeled benzene and labeled cumene (a) and unlabeled cumene and labeled benzene (b) over H-ZSM-11 (benzene/cumene = 2) [62].

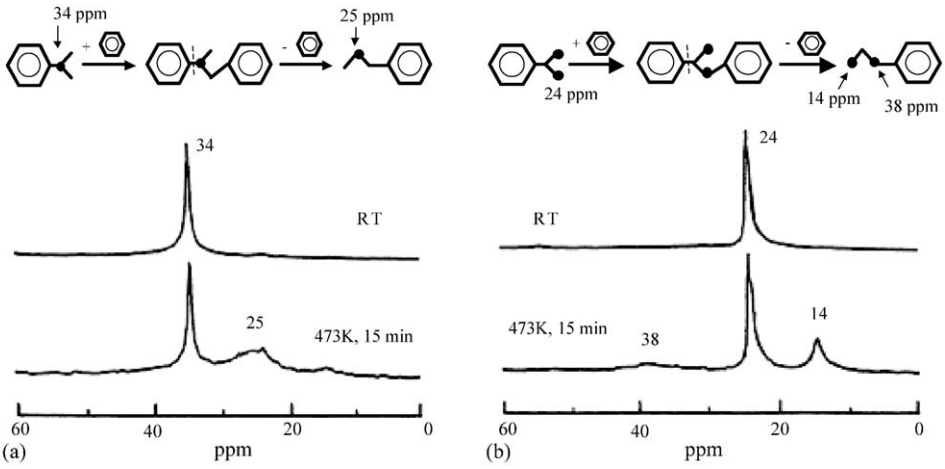

Fig. 10. Aliphatic regions of ^{13}C MAS NMR spectra observed before and after reaction of cumene α-^{13}C (a) and cumene β-^{13}C (b) with benzene at 473 K over H-ZSM-11 (benzene/cumene = 8) [40].

5. Skeletal isomerization of the alkyl chain

Further reaction step, which takes place at reaction temperatures higher than 473 K, involves skeletal isomerization in alkyl chain of alkylaromatic compounds. This reaction occurs only for limited class of alkylbenzenes, including more than three carbon atoms in their alkyl chains. The central question, which rose during the discussion of the mechanism of this reaction, was whether it occurs intra- or intermolecularly [29,64–67]. This question was best answered by in situ tracing MAS NMR techniques.

Such approach was applied for the investigation of cumene–*n*-propylbenzene (NPB) isomerization in the presence of benzene over H-ZSM-11 [60–62]. Two experiments were carried out. In the first one, cumene labeled in the aromatic ring was used to follow the fate of the aromatic carbon atoms. The aromatic regions of the ^{13}C MAS NMR spectra obtained in this experiment are shown in Fig. 9a. The spectrum of initial unheated sample contained three lines: at 149 ppm, corresponding to cumene 1-^{13}C, at 128.5 ppm, ascribed to cumene 3,5-^{13}C, and benzene-^{13}C and at 126.5 ppm attributed to cumene 2,4,6-^{13}C. After heating the sample for 60 min, the conversion of cumene to NPB estimated from the aliphatic part of the spectrum was more than 50%; meanwhile, the line at 149 ppm, corresponding to cumene 1-^{13}C, disappeared. However, the line at

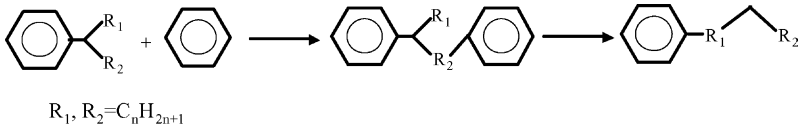

Fig. 11. Mechanism proposal for skeletal isomerization of alkyl chain in alkylaromatic compounds.

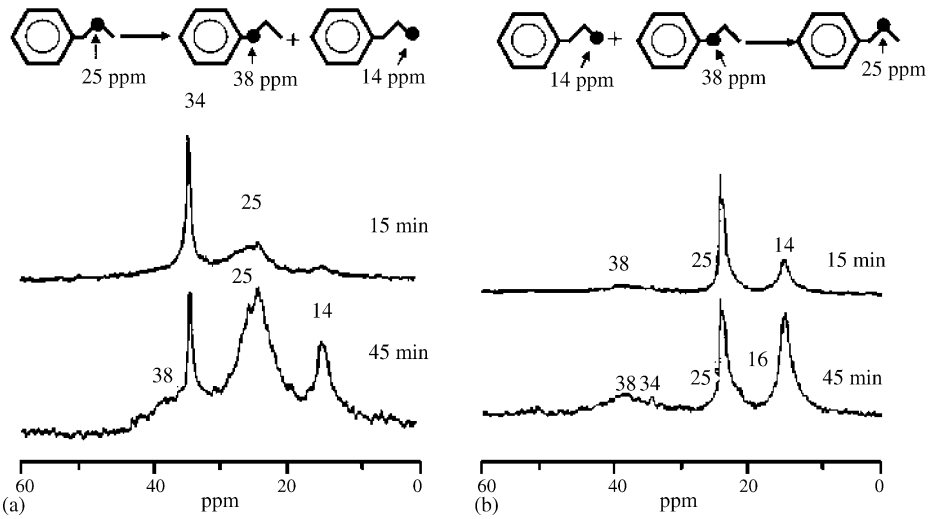

Fig. 12. ^{13}C scrambling in NPB observed in course of cumene α-^{13}C – NPB β-^{13}C (a) and cumene β-^{13}C – NPB α-^{13}C (b) transformations by in situ ^{13}C MAS NMR over H-ZSM-11 [62].

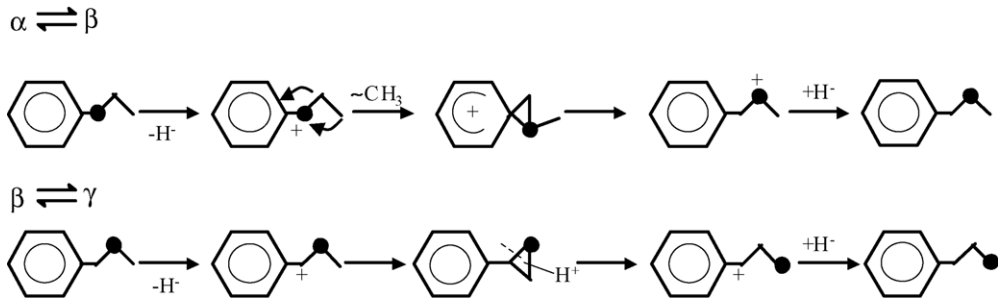

Fig. 13. Mechanism proposals for nonskeletal rearrangements of alkyl chain in NPB.

143 ppm corresponding to NPB 1-^{13}C was not observed. The complete disappearance of the ^{13}C-1 resonance of cumene and the absence of NPB labeled in the aromatic ring pointed to the intermolecular mechanism of the cumene–NPB isomerization.

Similarly, when using labeled benzene and unlabeled cumene, a benzene–NPB aromatic ring label transfer was evidenced by the appearance of the resonance at 143 ppm (Fig. 9b). This confirmed unambiguously the intermolecular character of cumene isomerization.

The intermolecular mechanism of the isomerization reaction was further detailed by experiments with cumene labeled in the alkyl chain. The analysis of ^{13}C label distribution in the alkyl chain of the primary products of cumene isomerization allowed to discriminate between monomolecular S_{N1} mechanism including dealkylation/alkylation steps and bimolecular S_{N2} mechanism involving formation of 1,2-diphenylpropane intermediate. The aliphatic regions of the ^{13}C MAS NMR spectra obtained during the reaction of cumene α-^{13}C and cumene β-^{13}C are shown in Fig. 10. The initial spectra contained single resonances either at 34 ppm (Fig. 10a) or at 24 ppm (Fig. 10b), corresponding to cumene labeled either at α- or at β-positions, respectively. Heating the samples at 473 K for 15 min led to the conversion of cumene α-^{13}C into NPB β-^{13}C (25 ppm) and cumene β-^{13}C into NPB α-^{13}C (38 ppm) and NPB γ-^{13}C (14 ppm), the latter two being obtained in equal amounts. This observation suggested that isomerization proceeds via intermediacy of diphenylpropane structure as shown in Fig. 10. In this mechanistic pathway, the ^{13}C label should be necessarily transferred into β-position of NPB in the case of starting cumene α-^{13}C and into α- and γ-positions in the case of starting cumene β-^{13}C. On the contrary, dealkylation/alkylation S_{N1} route should lead to statistical distribution of ^{13}C label in the alkyl chain of NPB.

Further evidences for S_{N2} mechanism of cumene–NPB isomerization were obtained during in situ ^{13}C MAS NMR study of cumene transformations over mordenite catalysts [61]. The weak resonance line at ca. δ = 146.1 ppm appearing in ^{13}C MAS NMR spectra at the onset of NPB formation and disappearing afterwards was attributed to 1,2-diphenylbenzene intermediate species.

The mechanism proposed on the basis of in situ MAS NMR results for skeletal isomerization of alkyl chain in alkylaromatic compounds is presented in Fig. 11.

6. Nonskeletal rearrangements in the alkyl chain

Nonskeletal (nonbranching) rearrangements in the alkyl chain include scrambling of carbon or hydrogen atoms in the alkyl chain and therefore can be followed only by label tracing techniques. In this respect, ^{13}C MAS NMR appears to be superior technique due to several reasons. Firstly, low natural abundance of isotope ^{13}C leads to the possibility of selective enrichment of specific positions of the molecule with ^{13}C. Secondly, the ability

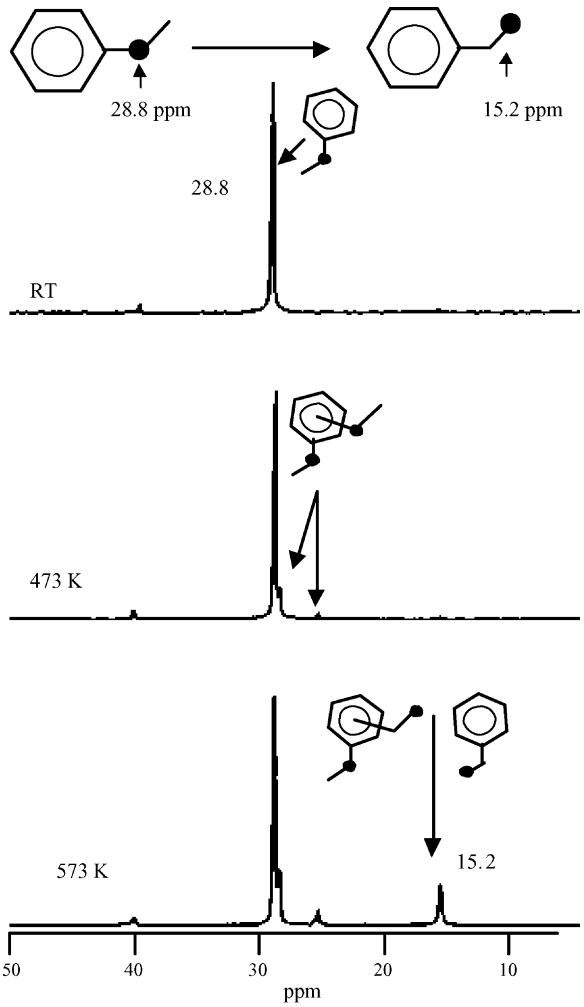

Fig. 14. ^{13}C MAS NMR spectra observed before and during the reaction of ethylbenzene α-^{13}C over H-MOR [63].

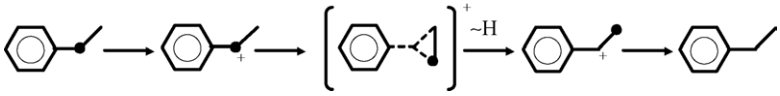

Fig. 15. Mechanism proposal for nonskeletal rearrangement of ethylbenzene [63].

of ^{13}C MAS NMR to distinguish unambiguously between carbon atoms in different positions of alkyl chain allows tracing the fate of these specifically labeled carbons during the time course of the reaction. Finally, the possibility to obtain quantitative information on the label distribution gives unique information on the reaction mechanisms.

Using in situ ^{13}C MAS NMR tracing technique, it was found that nonskeletal rearrangement in the alkyl chain of aromatic compounds is a slower reaction step in comparison with skeletal rearrangement. This was demonstrated in the example of cumene–NPB isomerization and ^{13}C label scrambling in the alkyl chain of NPB [60,62]. As it was shown above (Fig. 10), cumene–NPB isomerization is obeying S_{N2} mechanism, according to which the ^{13}C label from cumene α-^{13}C is selectively transferred into β-position of NPB and from cumene β-^{13}C into α,γ-positions of NPB. Heating of the sample at 473 K for another 30 min resulted in further cumene transformation into NPB (Fig. 12). Besides that, ^{13}C scrambling in NPB was observed as evidenced by appearance of NPB α,γ-^{13}C in the former case (Fig. 12a) and NPB β-^{13}C in the latter (Fig. 12b).

To account for α–β and β–γ scrambling in NPB, two mechanisms were proposed (Fig. 13) [60,62]. The former was reported previously for NPB rearrangement over $AlCl_3$ at 373 K [68]. It involves the removal of the benzylic hydrogen, followed by methyl migration, leading to phenonium ion as shown in Fig. 13. Phenonium ion rearranges preferentially towards NPB β-^{13}C. In the other mechanism accounting for β–γ scrambling, the first step also leads to the benzylic carbocation, whereas the rearrangement proceeds towards protonated phenylcyclopropane. Preferential α–β cleavage of protonated phenylcyclopropane may account for γ–β scrambling in NPB.

Another example of ^{13}C scrambling in alkyl chain was reported in [63] for ethylbenzene α-^{13}C rearrangement over mordenite catalysts (Fig. 14). The first reaction step observed at 473 K was formation of diethylbenzene with the ^{13}C label retained at the α-position of alkyl chain. Further heating at 573 K led to ^{13}C label transfer from α- to β-position. To account for this observation, the authors proposed mechanism (Fig. 15) similar to α–β scrambling in NPB (Fig. 13). However, instead of phenonium ion they suggested intermediate with two-electron–three-center bond.

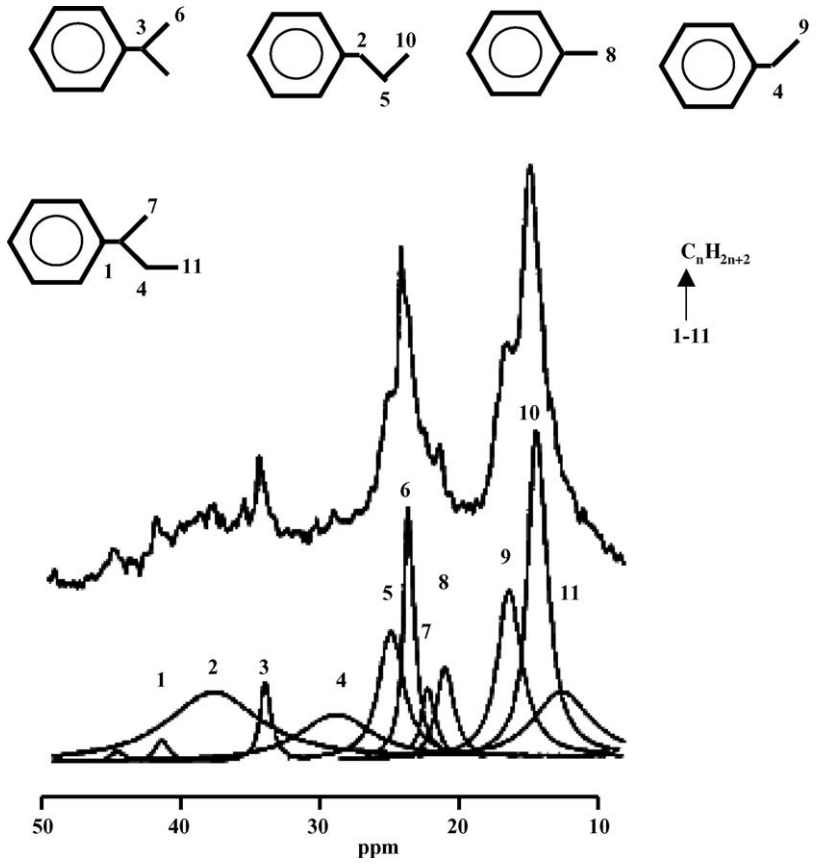

Fig. 16. Decomposed ^{13}C MAS NMR spectrum observed after the reaction of cumene α-^{13}C with benzene over H-ZSM-11 at 473 K [62].

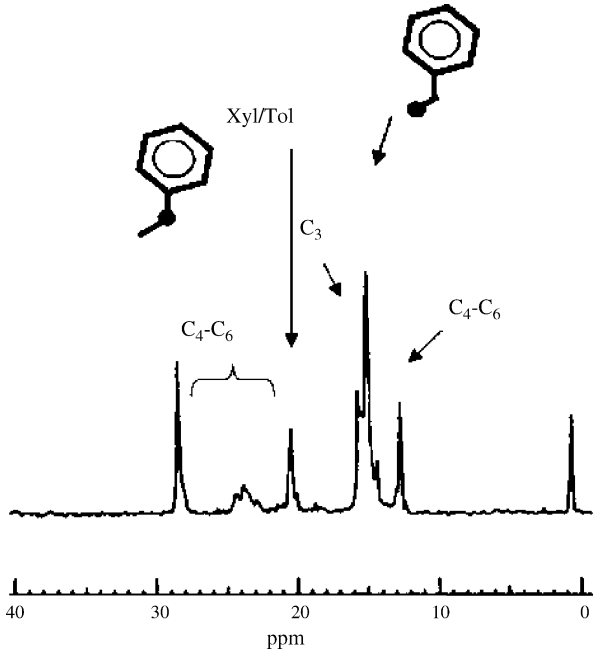

Fig. 17. ^{13}C MAS NMR spectrum observed after the reaction of ethylbenzene α-^{13}C over HMOR at 723 K [63].

7. Dealkylation and fragmentation

The final spectrum obtained in the course of cumene transformation over H-ZSM-11 catalyst is presented in Fig. 16. It can be decomposed at least into 11 lines as shown in Fig. 16: lines 2, 5 and 10 being ascribed to NPB alkyl chain atoms, 3 and 6 to cumene, 8 to toluene, 4 and 9 to ethylbenzene and 1, 4, 7 and 11 to *sec*-butylbenzene. Besides that, the NMR lines corresponding to C_3–C_6 aliphatic hydrocarbons can also contribute to the same spectral region. The observed products suggest that at higher reaction times dealkylation, fragmentation and dealkylation/alkylation endow to the overall reaction pathway.

Similarly, in the study of ethylbenzene transformation over mordenite catalysts, toluene, ethylbenzene and C_3–C_6 aliphatic hydrocarbons were found as the major products (Fig. 17) pointing to dealkylation, fragmentation and dealkylation/alkylation reactions as the final steps of transformations [63].

It was proposed [69,70] that fragmentation occurs via S_{N2} mechanism similar to transalkylation and skeletal isomerization pathways. In this case, however, alkyl shift in the diphenylalkane intermediate is required to account for the reaction products observed (Fig. 18). Another mechanism, which can also account for fragmentation products, involves dealkylation, oligomerization of the olefin formed, cracking of the oligomer and alkylation of benzene with the fragments formed (Fig. 19). This mechanistic pathway also explains the formation of other alkylbenzenes and C_3–C_6 aliphatic hydrocarbons. It can also account for transalkylation, disproportionation, skeletal isomerization and ^{13}C scrambling. However, ^{13}C MAS NMR investigations suggest that this mechanistic route contributes to the overall reaction pathway only at high contact times and elevated temperatures.

8. Effect of zeolite structure

The analysis of the influence of zeolite type on the mechanism of alkylbenzenes transformations has demonstrated that the dominating factor controlling the reaction pathway is zeolite geometry [69,70]. On medium pore zeolites (H-ZSM-5 and H-ZSM-11), the slimmest 1,2-diphenyl propane intermediate is preferentially formed during cumene transformation (Fig. 20). The energetically unfavorable hydride abstraction from β-position of cumene, required for its formation, can be compensated by confinement (nest) effect [71] within the channels of H-ZSM-11. This can explain the 10-fold increase in NPB selectivity on medium pore zeolites with respect to large pore zeolite materials. On the contrary, on large pore zeolites (mordenite, faujasite and beta), energetically favorable but more bulky intermediates: 2,2-diphenylpropane in the case of cumene and 1,1-diphenypropane in the case of *n*-propylbenzene, can be formed. These intermediates account for

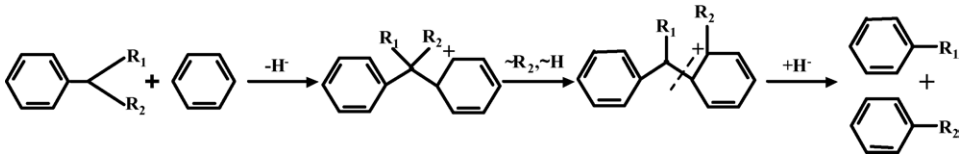

Fig. 18. Mechanism proposal for fragmentation of alkylaromatic compounds.

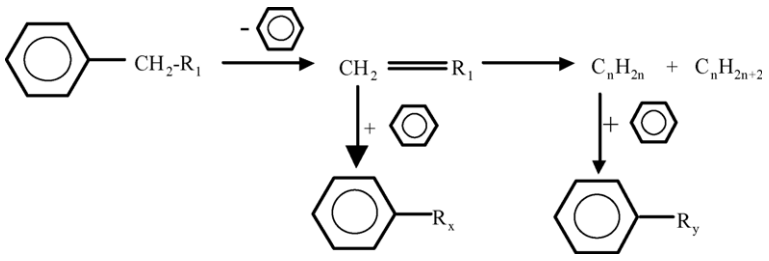

Fig. 19. Mechanism proposal for dealkylation/alkylation reactions.

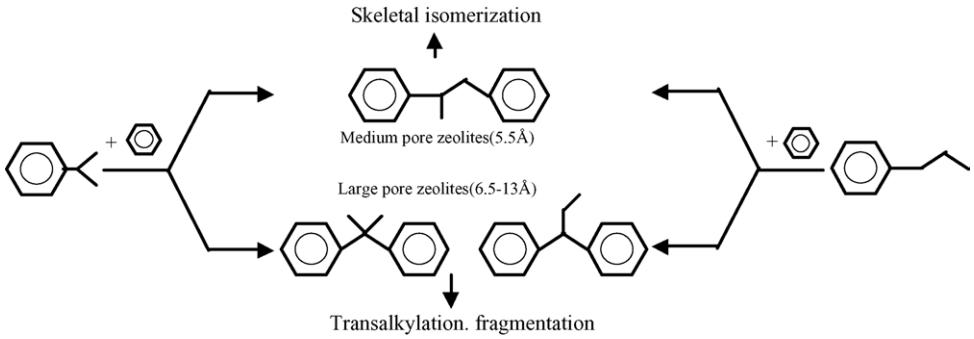

Fig. 20. Transformation of propylbenzenes over different zeolite catalysts.

transalkylation and fragmentation pathways, which predominate on this type of catalysts.

9. Conclusions

The main reaction pathways observed during alkylbenzene transformations over zeolite catalysts include exchange between zeolite protons and hydrogen atoms of aromatic ring and alkyl chain; transalkylation, disproportionation, skeletal isomerization, nonskeletal rearrangements, fragmentation and dealkylation/alkylation pathways. In situ MAS NMR pointed to the following mechanisms of these pathways:

- concerted mechanism of exchange between zeolite protons and protons of aromatic ring involving simultaneous cleavage of O–H bond in zeolite bridging OH group and formation of O–H bond between hydrogen atom of aromatic ring and the neighboring oxygen atom of zeolite;
- dealkylation/alkylation mechanism of exchange between zeolitic protons and protons of alkyl chain;
- two mechanisms of transalkylation and disproportionation involving intermolecular S_{N2} mechanism via bimolecular intermediates, in which aromatic rings are bridged by a C atom of the alkyl group and concerted mechanism of alkyl shift proceeding via eight member cyclic transition state;
- intermolecular mechanism of skeletal isomerization proceeding via intermediacy of diphenylalkane structure;
- intramolecular rearrangements of alkyl chain including protonated phenylcyclopropane intermediates;
- dealkylation/alkylation pathway involving elimination of alkyl group, oligomerization of the olefin formed, cracking of the oligomer and alkylation of aromatic compounds with the fragments formed;
- two mechanisms of fragmentation: intermolecular S_{N2} mechanism with intermediate diphenylalkane formation followed by alkyl shift; dealkylation/alkylation mechanism.

Hydrogen exchange, transalkylation and disproportionation pathways require mild conditions ($T = 295$–473 K, weak acidity), while skeletal and nonskeletal rearrangements of alkyl chain as well as fragmentation and dealkylation/alkylation steps require more severe conditions ($T > 473$ K, strong acid sites). The analysis of the influence of zeolite type on the mechanism of alkylbenzenes transformations has demonstrated that the dominating factor controlling the reaction pathway is zeolite geometry.

The results illustrated the potential of the in situ MAS NMR technique with the strategic labeling of organic reactants to bring most useful information on the details of the mechanism of heterogeneous catalytic reactions and to guide the design of more selective catalysis by showing the various unwanted side reactions occurring on the catalytic surface and therefore suggesting strategies to lower their extent.

Acknowledgments

I.I. Ivanova and N.S. Nesterenko thank Russian Foundation of Basic Research, Council for the Grants of Russian President (project NSh-1275.2003.3) and INTAS (project 03 51-5286) for the financial support. C. Fernandez thanks the FEDER and the Region Basse-Normandie for the financial support.

References

[1] J. Cejka, B. Wichterlova, Catal. Rev. Sci. Eng. 44 (3) (2002) 375.
[2] T.-C. Tsai, S.-B. Liu, I. Wang, Appl. Catal. A: Gen. 181 (2) (1999) 355.
[3] J.M. Serra, E. Guillon, A. Corma, J. Catal. 227 (2) (2004) 459.
[4] M.L. Poutsma, ACS Monograph, 1971, p. 431.
[5] P.A. Jacobs, Carboniogenic Activity of Zeolites, Elsevier, New York, 1977.
[6] D.C. Santilli, J. Catal. 99 (1986) 327.
[7] M. Guisnet, N.S. Gnep, NATO-A.S.I. 80 (1984) 571.
[8] D.H. Olson, W.O. Haag, ACS Symposium Series, vol. 248, 1984, p. 275.
[9] X. Rozanska, X. Saintigny, R.A. van Santen, F. Hutschka, J. Catal. 202 (1) (2001) 141.
[10] M. Guisnet, N.S. Gnep, S. Morin, Microporous Mesoporous Mater. 35–36 (2000) 47.
[11] E. Dumitriu, V. Hulea, S. Kaliaguine, M.M. Huang, Appl. Catal. A: Gen. 135 (1) (1996) 57.
[12] R. Bandyopadhyay, Y. Sugi, Y. Kubota, B.S. Rao, Catal. Today 44 (1–4) (1998) 245.
[13] R. Bandyopadhyay, P.S. Singh, R.A. Shaikh, Appl. Catal. A: Gen. 135 (2) (1996) 249.
[14] B. Wichterlova, J. Cejka, N. Zilkova, Microporous Mater. 6 (5–6) (1996) 405.
[15] S. Morin, P. Ayrault, S.E. Mouahid, N.S. Gnep, M. Guisnet, Appl. Catal. A: Gen. 159 (1–2) (1997) 317.
[16] F.E. Imbert, N.S. Gnep, P. Ayrault, M. Guisnet, Appl. Catal. A: Gen. 215 (1–2) (2001) 225.
[17] C.W. Jones, S.I. Zones, M.E. Davis, Appl. Catal. A: Gen. 181 (2) (1999) 289.
[18] R.Ch. Deka, R. Vetrivel, A. Miyamoto, Top. Catal. 9 (1999) 225.

[19] S. Morin, P. Ayrault, N.S. Gnep, M. Guisnet, Appl. Catal. A: Gen. 166 (2) (1998) 281.
[20] I. Wang, T.-C. Tsai, J. Catal. 133 (1992) 136.
[21] S. Morin, N.S. Gnep, M. Guisnet, Appl. Catal. A: Gen. 168 (1) (1998) 63.
[22] S. Morin, N.S. Gnep, M. Guisnet, J. Catal. 159 (2) (1996) 296.
[23] T.-C. Tsai, C.-L. Ay, I. Wang, Appl. Catal. 77 (2) (1991) 199.
[24] F. Thibault-Starzyk, A. Vimont, J.-P. Gilson, Catal. Today 70 (1–3) (2001) 227.
[25] R.C. Deka, R. Vetrivel, J. Catal. 174 (1) (1998) 88.
[26] E. Klemm, H. Schcidat, G. Emig, Chem. Eng. Sci. 52 (16) (1997) 2757.
[27] G. Mirth, J. Cejka, J.A. Lercher, J. Catal. 139 (1) (1993) 24.
[28] L. Forni, G. Cremona, F. Missineo, G. Bellussi, C. Perego, G. Pazzuconi, Appl. Catal. A: Gen. 121 (2) (1995) 261.
[29] B. Wichterlova, J. Cejka, J. Catal. 146 (2) (1994) 523.
[30] J.F. Haw, in: A.T. Bell, A. Pines (Eds.), NMR Techniques in Catalysis, Marcel Dekker, New York, 1994, p. 139.
[31] I.I. Ivanova, E.G. Derouane, Advanced Zeolite Science and Applications, Elsevier, Amsterdam, 1994, p. 357.
[32] W. Kolodziejski, J. Klinowski, in: A.T. Bell, A. Pines (Eds.), NMR Techniques in Catalysis, Marcel Dekker, New York, 1994, p. 361.
[33] A.G. Stepanov, Catal. Today 24 (3) (1995) 341.
[34] E.G. Derouane, H.Y. He, S. Hamid, D. Lambert, I.I. Ivanova, J. Mol. Catal. A Chem. 158 (1) (2000) 5.
[35] M. Hunger, J. Weitkamp, in: B.M. Weckhuysen (Ed.), In-Situ Spectroscopy of Catalysts, American Scientific Publishers, The Netherlands, 2004, p. 350.
[36] T. Xu, J.F. Haw, J. Am. Chem. Soc. 116 (22) (1994) 10188.
[37] J.F. Haw, Phys. Chem. Chem. Phys. 4 (22) (2002) 5431.
[38] X.W. Han, Z.M. Yan, W.P. Zhang, X.H. Bao, Curr. Org. Chem. 5 (10) (2001) 1017.
[39] I.I. Ivanova, Colloids Surf. Phys. Eng. Aspects 158 (1–2) (1999) 189.
[40] E.G. Derouane, H.Y. He, S.B. Derouane-Abd Hamid, I.I. Ivanova, Catal. Lett. 58 (1) (1999) 1.
[41] M.W. Anderson, J. Klinowski, Nature 339 (6221) (1989) 200.
[42] R.E. Taylor, L.M. Ryan, P. Tindall, B.C. Gerstein, J. Chem. Phys. 73 (1980) 5500.
[43] H. Pfeifer, D. Freude, M. Hunger, Zeolite 5 (1985) 274.
[44] V.M. Mastikhin, I.L. Mudrakovsky, A.V. Nosov, Prog. Nucl. Magn. Reson. Spectrosc. 23 (1991) 259.
[45] T.A. Carpenter, D.T.B. Tennakoon, C.J. Smith, D.C. Edwards, J. Magn. Reson. 68 (1986) 561.
[46] I.D. Gay, J. Magn. Reson. 58 (1984) 413.
[47] F. Rachidi, J. Reichenbach, L. Firlej, P. Bernier, M. Ribet, A. Aznar, G. Zimmer, M. Helmil, M. Mehring, Solid State Commun. 87 (1993) 547.
[48] E.J. Munson, D.B. Ferguson, A.A. Kheir, J.F. Haw, J. Catal. 136 (2) (1992) 504.
[49] J.F. Haw, B.R. Richardson, I.S. Oshiro, N.D. Lazo, J.A. Speed, J. Am. Chem. Soc. 111 (6) (1989) 2052.
[50] T. Xu, J.F. Haw, Top. Catal. 4 (1–2) (1997) 109.
[51] G.W. Haddix, J.A. Reimer, A.T. Bell, J. Catal. 106 (1) (1987) 111.
[52] M. Hunger, T. Horvath, J. Catal. 167 (1) (1997) 187.
[53] J.F. Haw, P.W. Goguen, T. Xu, T.W. Skloss, W.G. Song, Z.K. Wang, Angew. Chem. Int. Ed. 37 (7) (1998) 948.
[54] P. Goguen, J.F. Haw, J. Catal. 161 (2) (1996) 870.
[55] D. Ma, Y.Y. Shu, W.P. Znang, X.W. Han, Y.D. Xu, X.H. Bao, Angew. Chem. Int. Ed. 39 (16) (2000) 2928.
[56] M. Hunger, Catal. Today 97 (1) (2004) 3.
[57] L.W. Beck, T. Xu, J.B. Nicholas, J.F. Haw, J. Am. Chem. Soc. 117 (46) (1995) 11594.
[58] I.I. Ivanova, V. Montouillout, N.S. Nesterenko, Ch. Fernandez, J.-P. Gilson, unpublished results, 2002.
[59] A. Corma, F. Llopis, J.B. Monton, J. Catal. 140 (2) (1993) 384.
[60] I.I. Ivanova, D. Brunel, J.B. Nagy, G. Daelen, E.G. Derouane, Stud. Surf. Sci. Catal. 78 (1993) 567.
[61] I.I. Ivanova, V. Montouillout, C. Fernandez, O. Marie, J.P. Gilson, Microporous Mesoporous Mater. 57 (3) (2003) 297.
[62] I.I. Ivanova, D. Brunel, J.B. Nagy, E.G. Derouane, J. Mol. Catal. 95 (3) (1995) 243.
[63] A. Philippou, M.W. Anderson, J. Catal. 167 (1) (1997) 266.
[64] D. Best, B.W. Wojciechowski, J. Catal. 47 (1977) 11.
[65] H.K. Beyer, G. Borbely, in: Proceedings of the 7th International Zeolite Conference, Elsevier, New York, 1986, p. 867.
[66] S. Fukase, B.W. Wojciechowski, J. Catal. 109 (1988) 180.
[67] J. Cejka, G.A. Kapustin, B. Wichterlova, Appl. Catal. A: Gen. 108 (2) (1994) 187.
[68] R.M. Roberts, J. Am. Chem. Soc. 79 (1950) 5484.
[69] N.S. Nesterenko, A.V. Smirnov, I.I. Ivanova, NATO-S.S. 560 (2001) 411.
[70] N.S. Nesterenko, A.V. Smirnov, I.I. Ivanova, B.V. Romanovsky, Book of Abstracts ‘‘EuropaCat-3’’, vol. 1, 1997, p. 246.
[71] E.G. Derouane, J. Catal. 100 (1986) 541.